

Structural evolution of massive early-type galaxies

Ludwig Oser¹, Thorsten Naab¹, Jeremiah P. Ostriker²,
Peter H. Johansson³

¹ Max-Planck-Institut für Astrophysik, Karl-Schwarzschild-Strasse 1, 85741, Garching, Germany

² Department of Astrophysical Sciences, Princeton University, Princeton, NJ 08544, USA

³ Department of Physics, University of Helsinki, Gustaf Hällströmin katu 2a, FI-00014 Helsinki, Finland

oser@mpa-garching.mpg.de

Abstract. We use a large sample of cosmological re-simulations of individual massive galaxies to investigate the origin of the strong increase in sizes and weak decrease of the stellar velocity dispersions since $z=2$. At the end of a rapid early phase of star-formation, where stars are created from infalling cold gas, our simulated galaxies are all compact with projected half-mass radii of $\lesssim 1$ kpc and central line-of-sight velocity dispersions of ≈ 262 km s⁻¹. At lower redshifts ($z < 2$) those galaxies grow predominantly by the accretion of smaller stellar systems and evolve towards the observed local mass-size and mass-velocity dispersion relations. This loss of compactness is accompanied with an increase of central dark matter fractions. We find that the structural evolution of massive galaxies can be explained by frequent minor stellar mergers, which is the dominant mode of accretion for our simulated galaxies.

Keywords. galaxies: formation, galaxies: evolution, methods: numerical

1. Introduction

When compared to systems at the present day, massive ($\approx 10^{11} M_{\odot}$) quiescent galaxies at redshift 2 are much more compact. Their half-mass radii are typically a factor of three to five times smaller (≈ 1 kpc) and their effective stellar densities are at least an order of magnitude higher (Bezanson *et al.* 2009). These results are supported by deep observations that cannot find faint, previously missed, stellar envelopes (Carrasco *et al.* 2010) as well as by dynamical mass estimates derived through velocity dispersion measurements. While these massive compact galaxies are common at redshift 2 among the quiescent galaxy population they are extremely rare in the present-day Universe, suggesting that today's massive early-type galaxies underwent significant structural evolution up to the present day.

We show here that the structural evolution of massive early-type galaxies can be understood as a consequence of the two-phase formation scenario (Oser *et al.* 2010, Johansson *et al.* 2012). The compact cores of massive galaxies form during an early rapid phase of dissipational in-situ star formation at $6 \gtrsim z \gtrsim 2$ fed by cold flows and/or gas rich mergers leading to large stellar surface densities. At redshift $z \sim 2$ the observed as well as simulated galaxies are compact ($R_e \sim 1$ kpc), more flattened and disk-like than their low redshift counterparts. The subsequent evolution is dominated by the addition of stars that have formed ex-situ, i.e. outside the galaxy itself. This accretion is dominated by minor mergers and provides an explanation for the structural evolution of massive galaxies. The early domination of in-situ star formation and the subsequent growth by stellar mergers is in agreement with semi-analytical models (De Lucia *et al.* 2006).

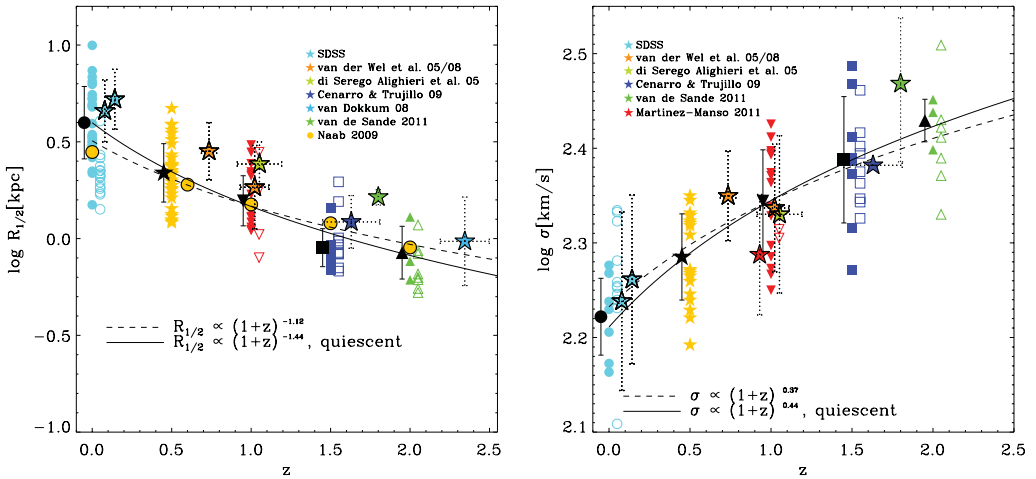


Figure 1. *Left:* Projected stellar half-mass radii of galaxies with stellar masses $M_* > 6.3 \times 10^{10} M_\odot$ as a function of redshift. The black symbols indicate the mean sizes at a given redshift with the error bars showing the standard deviation. The black lines show the result of a power law fit for all (dotted line) and quiescent (solid line and solid symbols) systems, respectively, in good agreement with the observed relations. Observational estimates from different authors are given by the solid star symbols. By $z=3$ all progenitor galaxies drop below our mass limit. *Right:* Evolution of the central stellar velocity dispersions, with open symbols for star-forming, and closed symbols for quiescent systems. We show the results for a power law fit with dashed (all) and solid (quiescent) lines. The simulated trend follows closely the observed relations (star symbols).

2. Size and velocity dispersion evolution

We present here the results obtained from 40 zoom-in re-simulations described in Oser *et al.* (2010) and Oser *et al.* (2012). These simulations follow the formation and evolution of a massive galaxy at high resolution with the help of a modified version of the TreeSPH code Gadget2 (Springel *et al.* 2005) including radiative cooling, star formation, supernovae feedback and a uniform UV radiation background. In an early dissipational phase, the stellar mass growth is primarily due to in-situ star formation. The baryonic mass is assembled in gaseous form and a significant amount of the potential energy is dissipated (Johansson *et al.* 2009). This leads to compact systems, with our simulated massive galaxies ($\sim 10^{11} M_\odot$) having half-mass radii of about 1 kpc (see left panel of Fig. 1). At later times, the simulated galaxies increase their stellar mass primarily by the accretion of smaller stellar systems, which – since this is a collisionless process – inevitably leads to a strong increase of the half-mass radii (Naab *et al.* 2009, Bezanson *et al.* 2009). The left panel of Fig. 1 shows the evolution of the average sizes of all galaxies with masses between $6.3 \times 10^{10} M_\odot$ and $5 \times 10^{11} M_\odot$ from redshift 2 up to the present day. We define galaxies with a specific star formation rate lower than $0.3/t_{hub}$, where t_{hub} is the Hubble time, as quiescent (solid symbols in Fig. 1). We fit the evolution of galaxy sizes with $R_{1/2} \propto (1+z)^\alpha$. We find $\alpha = -1.12$ for all and $\alpha = -1.44$ for the quiescent galaxies in agreement with the observed values.

At the same time, the central stellar velocity dispersions drop continuously with time from $\sim 260 \text{ km s}^{-1}$ at redshift 2 to $\sim 180 \text{ km s}^{-1}$ at the present day. We show the evolution of stellar velocity dispersions for our simulated galaxies along with some observations in the right panel of Fig. 1. We use again a power law ($\sigma_{1/2} \propto (1+z)^\beta$) to fit our results

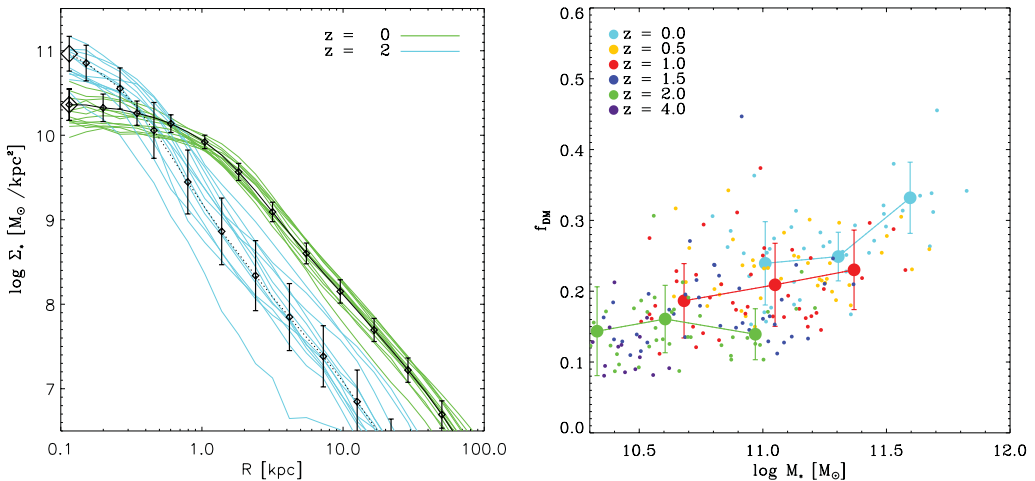


Figure 2. The left panel shows the stellar surface density profiles for the 13 most massive galaxies in our sample. We find that the stellar mass growth between redshift 2 and 0 is due to an increase in the stellar surface densities at larger radii. The right panel shows the evolution of central dark matter to stellar mass fractions. The dark matter fractions increase with mass as well as with time as a result of dissipational effects, being less important in systems of higher mass or later times.

and obtain values ($\beta = 0.37$ for all galaxies in our samples and $\beta = 0.44$ for the quiescent systems) similar to observational estimates (van de Sande *et al.* 2011).

Both the increase in sizes as well as the drop in velocity dispersion is expected as a result of dry mergers. Naab *et al.* (2009) and Bezanson *et al.* (2009) have shown that minor mergers are particularly effective in evolving these structural properties and we find that our simulated galaxies are indeed increasing their stellar mass at redshifts below zero by accreting gas-poor systems with an average mass ratio of 1:5 (Oser *et al.* 2012). The evolution of sizes and stellar velocity dispersions follows closely the analytical predictions obtained for collisionless merging.

3. Stellar surface density profiles and central dark matter fractions

In the presence of the dark matter halo potential, small satellites will, in general, be disrupted before they fall into the center of the host galaxy, and will therefore be added to the stellar distribution at large radii, leading to an inside-out growth (Hilz *et al.* 2013). The left panel of Fig. 2 shows the stellar surface density profiles for the 13 most massive galaxies in our sample at redshifts 2 and 0. We find as well that the stellar mass growth at late times is not taking place in the center but in the outer regions of the galaxies as a result of the accretion of smaller stellar systems. This agrees well with observed stellar surface density profiles at different redshifts (compare to Szomoru *et al.* 2012 or van Dokkum *et al.* 2010) and the overall change towards higher Sersic indices in the galaxy population with time (Buitrago *et al.* 2008). While the simulated galaxies are dominated inside the half-mass radius by stars that formed in-situ at redshift 2, we find that at the present day the stellar surface density at the half-mass radius is already higher for the accreted than for the in-situ created stars. Our simulation support the inside-out formation picture for massive galaxies.

Another result of the ongoing accretion events is an increase in the dark matter to stellar mass ratio inside of one effective radius. This is not merely due to the increased

half-mass radii but is also a result of violent relaxation, see Hilz *et al.* (2012) for a detailed analysis of the change in binding energies of the different components in collisionless merger simulations. In the right panel of Fig. 2 we show the central dark matter fractions as a function of stellar mass at various redshifts. At early times when the galaxies are fed by cold streams and in-situ star formation is at its peak, the dark matter fractions are typically low ($f_{DM} \sim 0.1$ at $z = 4$). At later times, when the stellar growth results from dry stellar mergers, dark matter fractions are increasing up to 0.25 – 0.35 at the present day (Johansson *et al.* 2012). We find an additional trend with galaxy mass as the fraction of accreted stars is higher in galaxies of larger mass. Observations, although with large uncertainties, hint at the same trend (Barnabè *et al.* 2011).

References

- Barnabè, M., Czoske, O., Koopmans, L. V. E., Treu, T., & Bolton, A. S. 2011, *MNRAS*, 415, 2215
- Bezanson, R., van Dokkum, P. G., Tal, T., Marchesini, D., Kriek, M., Franx, M., & Coppi, P. 2009, *ApJ*, 697, 1290
- Buitrago, F., Trujillo, I., Conselice, C. J., Bouwens, R. J., Dickinson, M., & Yan, H. 2008, *ApJL*, 687, L61
- Carrasco, E. R., Conselice, C. J., & Trujillo, I. 2010, *MNRAS*, 405, 2253
- Hilz, M., Naab, T., & Ostriker, J. P. 2013, *MNRAS*, 429, 2924
- Hilz, M., Naab, T., Ostriker, J. P., Thomas, J., Burkert, A., & Jesseit, R. 2012, *MNRAS*, 425, 3119
- Johansson, P. H., Naab, T., & Ostriker, J. P. 2009, *ApJL*, 697, L38
- . 2012, *ApJ*, 754, 115
- Naab, T., Johansson, P. H., & Ostriker, J. P. 2009, *ApJL*, 699, L178
- Oser, L., Naab, T., Ostriker, J. P., & Johansson, P. H. 2012, *ApJ*, 744, 63
- Oser, L., Ostriker, J. P., Naab, T., Johansson, P. H., & Burkert, A. 2010, *ApJ*, 725, 2312
- Springel, V. 2005, *MNRAS*, 364, 1105
- Szomoru, D., Franx, M., & van Dokkum, P. G. 2012, *ApJ*, 749, 121
- van de Sande, J., *et al.* 2011, *ApJL*, 736, L9
- van Dokkum, P. G., *et al.* 2010, *ApJ*, 709, 1018